HHS Public Access

Author manuscript

J Endocrinol. Author manuscript; available in PMC 2018 August 01.

Published in final edited form as:

J Endocrinol. 2017 August ; 234(2): 217–232. doi:10.1530/JOE-17-0250.

Origin of a rapidly evolving homeostatic control system programming testis function

Pengli Bu[1,2,*], **Shintaro Yagi**[5,¶], **Kunio Shiota**[5,6], **S.M. Khorshed Alam**[1,2,†], **Jay L. Vivian**[1,2], **Michael W. Wolfe**[1,3], **M.A. Karim Rumi**[1,2], **Damayanti Chakraborty**[1,2,‡], **Kaiyu Kubota**[1,2,§], **Pramod Dhakal**[1,2], and **Michael J. Soares**[1,2,4,¥]

[1]Institute for Reproductive Health and Regenerative Medicine, University of Kansas Medical Center, Kansas City, KS 66160

[2]Department of Pathology and Laboratory Medicine, University of Kansas Medical Center, Kansas City, KS 66160

[3]Department of Molecular and Integrative Physiology, University of Kansas Medical Center, Kansas City, KS 66160

[4]Department of Pediatrics, University of Kansas Medical Center, Kansas City, KS 66160

[5]Laboratory of Cellular Biochemistry, Veterinary Medical Sciences/Animal Resource Sciences, The University of Tokyo, Tokyo, 113-8657, Japan

[6]Waseda Research Institute for Science and Engineering, Waseda University, Tokyo 169-8555, Japan

Abstract

Mammals share common strategies for regulating reproduction, including a conserved hypothalamic-pituitary-gonadal axis yet individual species exhibit differences in reproductive performance. In this report, we describe the discovery of a species-restricted homeostatic control system programming testis growth and function. *Prl3c1* is a member of the prolactin gene family and its protein product (PLP-J) was discovered as a uterine cytokine contributing to the establishment of pregnancy. We utilized mouse mutagenesis of *Prl3c1* and revealed its involvement in the regulation of the male reproductive axis. The *Prl3c1* null male reproductive phenotype was characterized by testiculomegaly and hyperandrogenism. The larger testes in the *Prl3c1* null mice were associated with an expansion of the Leydig cell compartment. *Prl3c1* locus is a template for two transcripts (*Prl3c1-v1* and *Prl3c1-v2*) expressed in a tissue specific pattern. *Prl3c1-v1* is expressed in uterine decidua, while *Prl3c1-v2* is expressed in Leydig cells of the

¥To whom correspondence may be addressed: msoares@kumc.edu.

*Present address: Department of Pharmaceutical Sciences, College of Pharmacy and Health Sciences, St. John's University, Queens, NY 11439

¶Present address: Advanced Life Science Institute, Inc., Hachioji, Tokyo, 192-0031, Japan

†Present address: Department of Biochemistry, Bangabandhu Sheikh Mujib Medical University, Dhaka, Bangladesh

‡Present address: Massachusetts General Hospital Cancer Center and Department of Medicine, Harvard Medical School, Charlestown, MA 02129

§Present address: Department of Obstetrics and Gynecology, Tokyo Medical University, 6-7-1 Nishishinjuku, Shinjuku-ku, Tokyo 160-0023, Japan

Declaration of interest: There is no conflict of interest that could be perceived as prejudicing the impartiality of the research reported.

testis. 5′RACE, chromatin immunoprecipitation, and DNA methylation analyses were used to define cell-specific promoter usage and alternative transcript expression. We examined the *Prl3c1* locus in five murid rodents and showed that the testicular transcript and encoded protein are the result of a recent retrotransposition event at the *Mus musculus Prl3c1* locus. *Prl3c1-v1* encodes PLP-J V1 and *Prl3c1-v2* encodes PLP-J V2. Each protein exhibits distinct intracellular targeting and actions. PLP-J V2 possesses Leydig cell static actions consistent with the *Prl3c1* null testicular phenotype. Analysis of the biology of the *Prl3c1* gene has provided insight into a previously unappreciated homeostatic setpoint control system programming testicular growth and function.

Keywords

Testis; Leydig cells; prolactin family; transposable elements

Introduction

The process of reproduction has elements of regulation that are well conserved among diverse mammalian species (Achermann and Jameson 1999; Matzuk and Lamb 2008). This is best illustrated by the hypothalamic-pituitary-gonadal (HPG) axis and the hormones used as messengers to control fertility (Achermann and Jameson 1999; Matzuk and Lamb 2008). Interestingly, reproductive function is also characterized by features that are seemingly unique to a species. These unique features represent a broad spectrum of biological processes associated with reproduction, including the regulation of gonadal size and function, gamete characteristics, the onset of puberty, sexual behavior, pregnancy, fecundity, as well as many others (Bronson 1989). Physiological impacts of these species-specific traits can be robust and have profound effects on reproductive fitness. Thus, on a backbone of a highly conserved reproductive axis there are prominent differences in reproductive performance among species.

The testis is regulated by a conserved homeostatic pathway involving the hypothalamus and pituitary (Desjardins 1978; Hedger and de Kretser 2000); yet exhibits striking species-specific characteristics (Fawcett et al. 1973; Kenagy and Trombulak 1986; Short 1997). Within the conserved regulatory pathway, the hypothalamus and pituitary produce gonadotropin releasing hormone (GnRH) and gonadotropins (luteinizing hormone, LH; follicle stimulating hormone, FSH), respectively. GnRH regulates gonadotropin biosynthesis and secretion while LH and FSH act to regulate the growth and function of the testis (Hedger and de Kretser 2000; Matzuk and Lamb 2008). LH drives Leydig cell production of testosterone (Hedger and de Kretser 2000), which acts on an array of downstream targets to promote function of the entire male reproductive axis, including stimulating spermatogenesis, sperm maturation and transport, and male sexual and social behaviors (Desjardins 1978). FSH acts together with testosterone to promote sperm production (McLachlan *et al.* 1996; Matzuk and Lamb 2008). Homeostasis is achieved through a negative feedback system of testicular hormone action at the hypothalamus and pituitary to modulate the output of GnRH and gonadotropins, respectively (Amory and Bremner 2001; Tilbrook and Clarke 2001). These conserved elements of the male reproductive regulatory pathway have been effectively modeled in the mouse (Matzuk and Lamb 2008) but do not

account for the species diversity in testicular size and function in mammals (Kenagy and Trombulak 1986; Short 1997; Montoto *et al.* 2011, 2012). In some mammals, the size of the testis can represent as much as 8 percent of body mass, whereas in other mammals the testis contributes to less than 0.1 percent of body mass (Kenagy and Trombulak 1986; e.g. *Gerbilliscus afra*, 8.4%; *Mesocricetus auratus*, 2.9%; *Ovis aries*, 0.9%; *Mus musculus*, 0.8%; *Macaca mulatta*, 0.7%; *Bos taurus*, 0.1%; *Homo sapiens*, 0.08%). Testis size correlates with contributions of Leydig cell and spermatogenic compartments and with their capacity to produce testosterone and sperm, respectively (Short 1997; Simmons and Fitzpatrick 2012; Birkhead 2000). Considerable species differences exist in sperm production. It has been proposed that sperm production relates to the mating system used by a species (monogamy versus polygyny versus polyandry), where sperm production and competition directly impact reproductive success (Short 1997; Simmons and Fitzpatrick 2012; Birkhead 2000). These extraordinary species differences in testis growth and function necessitate species-specific mechanisms modulating the function of the male reproductive axis. The origins of these species-specific reproductive traits are not yet fully appreciated.

In this report, we present the discovery of a rapidly evolving homeostatic control system contributing to the regulation of testis size and function in the mouse and provide insights into a mechanism employed to achieve species-specific reproductive traits.

Materials and Methods

Animals and tissue collection

C57BL/6 mice and testes from *M. spretus*, *M. caroli* and *M. pahari* were purchased from The Jackson Laboratory (Bar Harbor, Maine). Testicular RNA samples from C57BL/6, 129S1/Svlmj, AKR/J, BALB/cByJ, BTBRT + tf/J, C3H/HeJ, CAST/EiJ, DBA/2J, FVB/NJ, KK/HIJ, NOD/LtJ, NZW/LacJ, PWD/PhJ, WSB/EiJ, and SJL/J mouse strains were obtained from Dr. Curtis Klaassen (University of Kansas Medical Center, Kansas City, KS). CD-1 mice and Brown Norway (BN) rats were purchased from Charles River Laboratories International (Wilmington, MA). Fischer 344 (F344) and Holtzman Sprague Dawley (HSD) rats were obtained from Harlan Laboratories (Indianapolis, IN). Animals were housed in an environmentally controlled facility with lights on from 0600 to 2000 h and were allowed free access to food and water. Timed pregnancies were generated by cohabitation of male and female mice. The presence of a seminal plug in the vagina was designated day 0.5 of gestation. Tissues for histological analysis were frozen in dry ice-cooled heptane and stored at −80°C until processing. Tissue samples for RNA or protein extraction were snap frozen in liquid nitrogen and stored at −80°C until processing. Male mice were individually housed for two weeks prior to the collection of blood samples from the orbital sinus under isoflurane anesthesia.

Prl3c1 mutant mouse embryonic stem (ES) cells were produced by the NIH Knock-Out Mouse Project (KOMP) and obtained from the KOMP Repository (www.komp.org; VG10539). The University of Kansas Medical Center Transgenic and Gene-targeting Facility (Kansas City, KS) injected the mutant ES cells into C57BL/6 blastocysts. Germline competent chimeras were generated on C57BL/6 background and the mutation was subsequently moved to a mixed background of C57BL/6 X CD-1. Genotyping was routinely

performed on genomic DNA isolated from tail biopsies using PCR with forward primers specific for the wild type allele (5′ CAGGGAATTCTTTGATTTGC 3′) and mutant allele (5′GCAATTGGACCGTTTGATCT 3′) and a common reverse primer (5′ ATCTGAGTTGCTGGCTTGGT 3′). Amplicons generated by the PCR reactions for the wild type and mutant alleles were 798 and 471 bp, respectively. All null mutant animals were generated on the mixed background using heterozygous × heterozygous breeding and wild type and null littermates were used in the experiments.

All experimentation with animals was performed in accordance with guidelines recommended by the National Institutes of Health (Bethesda, MD). The University of Kansas Animal Care and Use Committee approved protocols for the care and use of animals.

Fertility tests

Beginning at 2–2.5 months of age, male and female mice were cohabited. Mutant and wild type males were housed with multiple wild-type females; whereas, mutant and wild type females were paired with fertile wild type males. The presence of seminal plugs in the vagina were examined daily. Seminal plug positive females were sacrificed on day 9.5 of pregnancy and the number of viable conceptuses counted.

Serum hormone measurements

Serum testosterone and LH levels were measured by radioimmunoassay at the University of Virginia Center for Research in Reproduction Ligand Assay and Analysis Core (Charlottesville, VA). Details of the assay procedures can be found at http://www.medicine.virginia.edu/research/institutes-andprograms/crr/ligand-page. Serum FSH levels were measured using an FSH Milliplex MAP kit (Millipore).

Sperm quantification

Sperm preparations and quantifications were based on previously described procedures (Jimenez *et al.* 2010). The caudal portion of the epididymis along with vas deferens of adult mice were isolated and cut at various points with a razor blade to release sperm into pre-warmed modified Whitten's Medium (100 mM NaCl, 4.7 mM KCl, 1.2 mM KH_2PO_4, 1.2 mM $MgSO_4$, 5.5 mM glucose, 0.8 mM Na pyruvate, 4.8 mM lactic Acid, 20 mM HEPES and 1.7 mM $CaCl_2$, pH 7.3). Following a 10 min incubation at 37°C, sperm in the supernatant were counted with a hemocytometer.

Assessment of sperm motility

Wild type and *Prl3c1* null sperm were analyzed by CASA, using the Minitube Sperm Vision Digital Semen Evaluation system (version 3.5; Penetrating Innovations, Verona, WI), as previously described (Jimenez *et al.* 2010, 2011).

Seminiferous tubule staging and testicular compartment enrichment

Seminiferous tubule staging was determined according to criteria presented by Hess (Hess 1990). Testicular interstitium and seminiferous tubule enrichments were prepared as previously described (Dufau and Catt 1975). Briefly, decapsulated testes were transferred to DMEM/F12 Medium (Sigma-Aldrich, St. Louis, MO) supplemented with 2.5% fetal bovine

serum (FBS, Sigma-Aldrich), 5% horse serum (Sigma-Aldrich), 15 mM HEPES, and 0.25 mg/ml collagenase (type IV; Sigma-Aldrich, C-5138) and incubated at 37°C for 20 min with continuous rotation. After settling for 5 min at room temperature, supernatants were transferred to a new tube and left on ice. Pellets were resuspended in the same medium and incubated as described above for another 10 min. Supernatants were combined and centrifuged at 600 g for 8 min to collect Leydig cells. The enriched Leydig cell preparations were used as a source of RNA and genomic DNA.

Immunohistochemical and immunofluorescence staining

All histochemical staining was performed on 10 μm frozen sections. After fixation with Bouin's fixative at 4°C, testis sections were incubated overnight at 4°C with antibodies against cytochrome P450 side-chain cleavage enzyme (CYP11A1; 1:300) (Roby *et al.* 1991), MKI67 (Santa Cruz Biotechnology, Santa Cruz, CA; sc-15402, 1:100), or PLP-J (1:50) (Alam *et al.* 2008). Quantification of CYP11A1 immunostaining was obtained using the Automated Cellular Imaging System (San Juan Capistrano, CA). Confocal images were obtained with a Nikon C1 plus confocal system equipped with 543-nm HeNe, 488-nm Ar, and 405-nm diode lasers integrated into an Eclipse TE2000-U microscope with 20×/0.75 Plan Apochromat and 60×/1.40/0.21 oil Plan Apochromat objectives (Nikon Instruments, Inc., Melville, NY). Image acquisition was performed using Nikon EZ C1 software.

RNA analysis

RNA was extracted from tissues or cells using TRI Reagent (Sigma-Aldrich) according to the manufacturer's instructions. Reverse transcription and quantitative RT-PCR (qRT-PCR) were performed as previously described (Kent *et al.* 2010; Konno *et al.* 2010). Primer sequences used for RT-PCR and qRT-PCR are provided in Supplementary Table 1.

Rapid amplification of 5′ cDNA ends (5′ RACE)

Transcription start sites for *Prl3c1-v1* and *Prl3c1-v2* were determined with RNA isolated from anti-mesometrial uterine decidual tissues (gestation day 7.5) and enriched Leydig cell preparations using a 5′ RACE kit (Roche, Pleasanton, CA, 03353621001), according to the manufacturer's instructions. Primer sequences used in the 5′RACE: SP1-Rev568: 5′ CCACCTGTCAGGCTCGTTAT 3′; SP2-Rev518-495: 5′ GTAAAGCTTTTGCTCCCTCCAGAA 3′; SP3-Rev227-196: 5′ TGTGACGAGAAGAGGAAAGCAGATTGTCATAG 3′.

ChIP analysis

Decidual cell and enriched Leydig cell preparations were used as starting material for the ChIP analyses. Anti-mesometrial uterine decidual tissue was dissected from gestation day 7.5 implantation sites. Implantation sites were pooled from pregnant females. Immediately following dissection, the tissue was incubated in pre-warmed PBS supplemented with collagenase (type IV, 0.25 mg/ml, Sigma-Aldrich), trypsin (0.25 mg/ml, Invitrogen) and Dispase (2 units/ml, Worthington Biochemical, Lakewood, NJ) with continuous rotation at 37°C for 30 min. Decidual cells were collected from the dispersed cell suspensions by centrifugation at 600 g. Pellets were then washed with cold PBS and used for crosslinking

and lysis. ChIP analysis was performed using an antibody against RNA polymerase II (EMD Millipore, Billerica, MA; 05-623B) and the EZ-ChIP kit (EMD Millipore, 17–371) according to the manufacturer's instructions. Sonication of decidual genomic DNA was achieved using Bioruptor 300 (Diagenode, Belgium) yielding DNA fragments ranging in length from 300 to 600 bp (Bioruptor 300 settings: power, high; sonication, 20 seconds on and 50 seconds off, 22 cycles). For the Leydig cell ChIP, freshly isolated enriched Leydig cells from testes were pooled. Cells were washed with cold PBS and the ChIP performed using EZ-ChIP kit. Sonication of the enriched Leydig cell genomic DNA was achieved using Bioruptor 300 yielding DNA fragments ranging in length from 300 to 600 bp (Bioruptor 300 settings: power, high; sonication, 20 seconds on and 50 seconds off, 15 cycles). Primers used for the ChIP PCR analysis are provided in Supplementary Table 1.

DNA methylation analysis

DNA methylation was determined using bisulfite sequencing, direct sequencing, and MultiNA-Combined Bisulfite Restriction Analysis (COBRA).

Bisulfite sequencing—Bisulfite PCR products were purified with the Wizard SV Gel and PCR Clean-up System (Promega, Madison, WI). For direct sequencing, purified PCR products were used for sequencing reactions with primers used for bisulfite PCR. PCR products were cloned into pGEM-T Easy Vector (Promega). Up to 16 plasmid clones were amplified with the Templiphi DNA Amplification Kit (GE Healthcare) and sequenced. The data were processed using the Quantification Tool for Methylation Analysis (QUMA) website (http://quma.cdb.riken.jp/).

COBRA with MultiNA microchip—Genomic DNA (2 to 8 μg) was digested with EcoRV at 37°C overnight. The DNA was extracted with phenol/chloroform/isoamyl alcohol (PCI; 25:24:1), precipitated with ethanol, and dissolved in TE. Five hundred ng of the EcoRV-digested DNA were bisulfite-converted using EZ DNA Methylation-Direct Kit (Zymo Research, Irvine, CA), and eluted in M-Elution Buffer. One-fortieth of the DNA was used for PCR in 20 μl of a reaction containing 1× buffer, 1.5 mM $MgCl_2$, 0.2 mM dNTP, and 0.25 μM each of primers with BIOTAQ HS DNA Polymerase (Bioline, Taunton, MA) under the following conditions: denaturation at 95°C for 7 min, and 43 cycles of 1 min at 94°C, 30 sec at 58–61°C, and 1 min at 72°C, followed by 10 min at 72°C. Primer sequences are listed in Supplementary Table 3. One-fifth of the PCR product was digested with HpyCH4IV or TaqI in 20 μl at 37°C overnight and analyzed with MultiNA Microchip Electrophoresis System (Shimadzu, Kyoto, Japan). The methylation level was calculated as previously described (Sato *et al.* 2010).

Cell culture

MA-10 mouse Leydig cells (a gift from Dr. Mario Ascoli, University of Iowa, Iowa City, IA) were cultured in Waymouth's MB752/1 Medium (Life Technologies) supplemented with 15% horse serum (Sigma-Aldrich) and 20 mM HEPES. TM3 mouse Leydig cells (ATCC, Manassas, VA; CRL-1714) were cultured in DMEM/F12 Medium (Sigma-Aldrich) supplemented with 2.5% fetal bovine serum (FBS, Sigma-Aldrich), 5% horse serum, 15 mM HEPES. MLTC-1 mouse Leydig cells (ATCC, CRL-2065) were cultured in RPMI 1640

Medium (Life Technologies) supplemented with 10% FBS. COS-7 African green monkey kidney fibroblast-like cells (ATCC, CRL-1651) were cultured in DMEM Medium (Life Technologies) supplemented with 10% FBS. Cell number was assessed using MultiTox-Fluor Multiplex Cytotoxicity Assay (Promega, G9200), according to the manufacturer's instructions.

Plasmids, transfection, subcellular fractionation, and western blotting

A *Prl3c1-v1* cDNA was obtained from Open Biosystems (Thermo Scientific, Pittsburgh, PA) and used as a template for PCR amplification of the coding sequence for *Prl3c1-v2. Prl3c1-v1* and *Prl3c1-v2* coding sequences were cloned into *pCMV6-Entry* (Origene, Rockville, MD) using *XhoI* and *EcoRV* restriction sites generating constructs with inframe C-terminal FLAG tags. The accuracy of both expression constructs was confirmed by DNA sequencing. Cells were transfected with an empty *pCMV6-Entry* vector or with vectors containing tagged *Prl3c1-v1* or *Prl3c1-v2* using Lipofectamine 2000 (Life Technologies). Cells were harvested for subcellular fractionation 48 h after transfection using NE-PER Nuclear and Cytoplasmic Extraction Reagents (Thermo Scientific, 78833) according to the manufacturer's instructions. Transfection efficiencies for MLTC-1, MA-10, TM3, and COS7 cells were 72.2 ± 7.1%, 62.0 ± 6.2%, 70.0 ± 6.4%, and 88.0 ± 4.2%, respectively. Western blotting procedures were performed as previously described (Deb *et al.* 1993). PLP-J V1-FLAG and PLP-J V2-FLAG were detected with antibody to the FLAG tag (Sigma-Aldrich, F3165, 1:2,500). Antibodies against Histone H3 (Abcam, Cambridge, MA; ab94817, 1:10,000) and GAPDH (EMD Millipore, Billerica, MA; MAB374, 1:7,500) were used as controls to monitor the integrity of the subcellular fractionation.

Statistical analysis

Differences between two groups were assessed by Student's *t* test. Data are presented as the mean ± standard error of the mean. *P* values less than 0.05 are considered statistically significant.

Results

PRL family gene expansion and *Prl3c1* gene disruption

Gene duplication represents a potential mechanism for acquisition of species-specific physiological traits (Ohno 1970; Kaessmann 2010). Several genes associated with reproduction have undergone expansions (Rawn and Cross 2008). Prolactin (PRL), a well-conserved hormone/cytokine best known for its actions on the reproductive tract and mammary gland (Freeman et al. 2000; Bachelot and Binart 2007), has undergone species-specific gene duplication (Soares 2004; Soares *et al.* 2007). In some species, the ancestral PRL served as a template for the birth of new genes (mouse, rat, and cow), while in other species, exemplified by the human, cat, and dog, only the PRL ortholog is present in the genome (Soares 2004; Soares *et al.* 2007). Mutagenesis experiments suggested that a driving force in the expansion of the mouse PRL family was associated with pregnancy-dependent adaptations to physiological stressors (Ain *et al.* 2004; Soares 2004; Alam *et al.* 2007; Soares *et al.* 2007). Mouse *Prl* contributes to the regulation of pregnancy and mammary gland development (Horseman *et al.* 1997), whereas *Prl4a1* and *Prl8a2* possess roles in

adaptations to environmental challenges during pregnancy (Ain *et al.* 2004; Alam *et al.* 2007). *Prl3c1* encodes a protein called PRL like protein-J (PLP-J, also referred to as PRL3C1) and was originally identified in uterine decidua of the mouse and rat (Hiraoka *et al.* 1999; Ishibashi *et al.* 1999; Toft and Linzer 1999; Dai *et al.* 2000). PLP-J was shown to act as a heparin-binding cytokine contributing to growth regulation of cells within the uterus (Alam *et al.* 2008). These observations prompted the generation of mice possessing a null mutation at the *Prl3c1* locus, with the expectation of a pregnancy-related phenotype. The entire coding sequence of *Prl3c1* was replaced with an inframe β-galactosidase (LacZ) cassette (inserted at the ATG codon in the first exon) followed by a neomycin resistance cassette (Fig. 1A,B). The mutation was successfully transmitted through the germline.

Assessment of fertility

Prl3c1 null and wild type males exhibited similar fertility. All wild type males successfully impregnated wild type females (n=13 males generated n=28 seminal plug positive females, leading to 28 pregnancies; 100% success rate). *Prl3c1* null males also successfully impregnated wild type females (n=12 males generated n=24 seminal plug positive females, leading to 19 pregnancies; 79% success rate). All wild type females (n=13) effectively mated during cohabitation with wild-type males, which led to 12 pregnancies (n=12; litter size: 10.5 ± 0.4). The *Prl3c1* null females were subfertile. Only 58% (7 of 12), mated during cohabitation with wild type males and only 57% of the seminal plug-positive females were pregnant on gestation day 9.5 (n=4; litter size: 11.0 ± 3.9). In this report, we focus our analysis on the reproductive tract phenotype of *Prl3c1* null male mice.

Prl3c1 null mice have an altered male reproductive tract phenotype

Mice possessing a null mutation at the *Prl3c1* locus exhibited an unexpected male reproductive tract phenotype. At the time of weaning *Prl3c1* null male mice exhibited precocial development of the scrotal region (Fig. 1C). The scrotal anomaly was associated with large testes (Fig. 1D,E; Supplementary Table 3). Since body weights were significantly greater in the *Prl3c1* mutant males, we have included both relative and absolute testis measurements (Fig. 1E; Supplementary Table 3). Within the testis, interstitial compartments from *Prl3c1* deficient mice were significantly expanded and contained more MKI67-positive cells when compared to testes of wild type mice (Fig. 1F–M). Postnatal testis development is associated with an initial expansion and then a decline in Leydig cell progenitors (proliferative population) and a subsequent increase in adult Leydig cells (post-mitotic population) (Benton *et al.* 1995; Ge *et al.* 2005; Chen *et al.* 2010; **Stanley *et al.* 2010**). Most interestingly, several Leydig cell progenitor-associated transcripts remained elevated in the adult *Prl3c1* null testis (Fig. 2A). Conversely, an indicator of adult Leydig cells, *Hsd3b6*, failed to exhibit the expected developmental increase in the adult *Prl3c1* null testis and instead, *Hsd3b1*, another 3β hydroxysteroid dehydrogenase isoform with similar substrate specificity was elevated in the adult *Prl3c1* null testis (Fig. 2B). Two transcripts encoding 5α reductase were decreased in *Prl3c1* null testes (Fig. 2B). Other testicular transcripts encoding proteins participating in steroidogenesis were more modestly affected by *Prl3c1* disruption (Fig. 2C). Indices of testicular function were also examined. Serum testosterone levels were elevated, androgen-responsive tissues were hyper-stimulated, and sperm production was significantly greater in *Prl3c1* null versus wild type male mice (Fig. 3;

Supplementary Table 3). Diameters of seminiferous tubules and the ratio of stage VIII seminiferous tubules to the total numbers of seminiferous tubules per cross-sectional area of the testis were similar in *Prl3c1* null and wild type testis; however, the *Prl3c1* null testes had significantly more seminiferous tubules per cross-section than did the wild type testis (wild type: 228.2 ± 7.2 versus *Prl3c1* null: 347.7 ± 5.8, P<0.001). Wild type and *Prl3c1* null sperm exhibited similar patterns of motility. Seminal vesicle glands continued to grow as the *Prl3c1* null mice aged and showed pathologic changes, including exhibiting regions of necrosis and hemorrhage (Fig. 3C,D). Overall, the evidence supported a hyperfunctionality of the *Prl3c1* null testis driven by an alteration of the developmental maturation of Leydig cells. *Prl3c1* mutant Leydig cells retain their ability to proliferate and functionally generate a hyperandrogenic condition.

A linkage between the *Prl3c1* null phenotype and *Prl3c1* gene expression was explored. In a survey of several tissues from wild type male mice, *Prl3c1* transcripts were prominently detected in the testis and preferentially localized to the interstitial compartment within the testis, as was PLP-J immunoreactivity (Fig. 4A–C). LacZ activity corresponding to activation of the *Prl3c1* gene in heterozygous *Prl3c1* mutant testes was co-localized with CYP11A1 immunoreactivity, demonstrating *Prl3c1* gene activation specifically within Leydig cells (Fig. 4D). Localization of *Prl3c1* to Leydig cells of the mouse testis has been previously reported (Yang *et al.* 2014). Testicular *Prl3c1* expression showed a developmental ontogeny similar to adult Leydig cell marker genes, including *Hsd3b6* (Fig. 5).

Collectively, the phenotype suggested that PLP-J expression by Leydig cells regulates programming of the setpoint for testicular growth and function. In the absence of a functional *Prl3c1* gene the setpoint for testicular size and functional output was increased.

The testicular homeostatic setpoint control system includes the pituitary

The normal core functions of the testis are driven by an efficient homeostatic interplay of hypothalamic and pituitary signals, which are responsive to the testicular output they control. Since LH is the primary driver of Leydig cell function and Leydig cells are hyperfunctional in the *Prl3c1* null mouse, we examined the contributions of LH to the *Prl3c1* null phenotype. Serum LH levels were higher in *Prl3c1* null mice, as was the *Lhb* transcript concentration of the pituitary (Fig. 6A,B). Elevations in LH prompted serum FSH and *Fshb* transcript measurements. Serum FSH levels did not differ between the genetic groups; however, *Fshb* transcript concentrations were significantly lower in pituitaries from *Prl3c1* null males (Fig. 6C,D). Thus, there is a potential contribution of the pituitary, and more specifically elevated circulating LH, to the regulation of the Leydig cell phenotype observed in the *Prl3c1* null testis. The male HPG axis appears to be operating in a unidirectional mode in *Prl3c1* null mice with a distorted setpoint for negative feedback modulation by gonadal testosterone.

The *Prl3c1* gene is a template for two transcripts

Prl3c1 transcripts expressed in uterine decidua and testes were compared and determined to be distinct, each utilizing different first exons driven by alternative promoters (Fig. 7). Decidual and Leydig cell *Prl3c1* transcription start sites and promoters were identified by 5′

RACE (Supplementary Fig. 1A,B) and chromatin immunoprecipitation (ChIP), using antibodies to RNA polymerase II (POL II; Fig. 7B), respectively. The two transcripts were operationally defined as *Prl3c1-v1* and *Prl3c1-v2* (Fig. 7C). The transcription start site for *Prl3c1-v1* was located 46 bp upstream of the ATG for *Prl3c1-v1*, whereas the transcription start site for *Prl3c1-v2* was located 136 bp upstream of the ATG for *Prl3c1-v2* (Supplementary Fig. 1A,B). An upstream promoter directs *Prl3c1-v1* transcription (Fig. 7B,C). The *Prl3c1-v1* transcript contains an upstream exon defined as Exon 1a and encodes a secreted protein previously characterized from the uterine decidua (Alam *et al.* 2008), which we refer to as PLP-J V1 (Fig. 7C). A second promoter, embedded within the first intron of the *Prl3c1* gene, directs *Prl3c1-v2* transcription (Fig. 7B,C). The *Prl3c1-v2* transcript contains an alternate first exon defined as Exon 1b and encodes a protein termed PLP-J V2 (Fig. 7C). Within the testis, the alternative promoter is operative in Leydig cells. This pattern of testicular *Prl3c1-v2* expression is conserved in fifteen different mouse strains (Supplementary Fig. 1C).

Origin of the testicular homeostatic setpoint control system

Transposable elements are sources of genetic information that have contributed to the evolution of the mammalian genome (Kaessmann 2010; Rebollo *et al.* 2012; Chuong *et al.* 2017). They are vestiges of viral infections and exist as repetitive sequences dispersed throughout the genome (Kidwell and Lisch 2001; Rebollo *et al.* 2012). Although the host organism has defense mechanisms for silencing transposable elements, in some cases these elements escape repression and contribute to the birth of new genes and regulatory information controlling gene transcription (Kidwell and Lisch 2001; Jern and Coffin 2008; Rowe and Trono 2011; Feschotte and Gilbert 2012; Rebollo *et al.* 2012; Chuong *et al.* 2017). Transposable element contributions to the regulation of reproduction have been described (Rebollo *et al.* 2012; Feschotte and Gilbert 2012; Emera and Wagner 2012; Chuong *et al.* 2017).

Comparison of mouse versus rat *Prl3c1* loci established a connection between the testicular homeostatic setpoint control system and the insertion of a composite transposable element within the mouse *Prl3c1* locus. The rat possesses a *Prl3c1* ortholog, which is expressed in uterine decidua (Hiraoka *et al.* 1999; Ishibashi and Imai 1999; Toft and Linzer 1999; Dai *et al.* 2000) but not in testes (Fig. 8A). Closer inspection of the rat *Prl3c1* gene revealed that it possesses a shorter first intron that lacks Exon 1b, which is characteristic of the mouse *Prl3c1-v2* transcript (Fig. 8B). The extended length of the first intron of mouse *Prl3c1* was attributed to the insertion of a composite transposable element consisting of two parts of an LTR-type element referred to as RMER17D_MM separated by a LINE element (L1 Mus_3 end; Fig. 8C). The RMER17D_MM element is restricted in its genomic distribution. Of the 4,977 RMER17D_MM insertion sites (80–100% sequence identity) within the mouse genome, 76.79% (3,823 copies) are located within intergenic regions, 23.2% (1,149 copies) in intronic regions, and 0.01% (5 copies) within exons. Insertion of the composite transposable element into the first intron of the mouse *Prl3c1* gene provides an alternative promoter and an alternative first exon (Exon 1b), structures absent from the rat *Prl3c1* locus.

Rapidly evolving testicular homeostatic setpoint control system

The rat is estimated to have diverged from the mouse approximately 25.2 million years ago (Mya) (Hedges *et al.* 2006). We reasoned that other *Mus* species sharing a closer evolutionary history with *M. musculus* (divergence from *M. musculus: M. spretus*, 1.8 Mya; *M. caroli*, 3.2 Mya; *M. pahari*, 7.9 Mya) (Guenet and Bonhomme 2003; Petkov *et al.* 2004; Keane *et al.* 2011) could provide additional insights into the evolutionary origin of this alternative *Prl3c1* transcript. Nucleotide sequences for the first intron of the *Prl3c1* gene corresponding to each of the four *Mus* species were determined and compared (Fig. 8D–F). *M. musculus* and *M. spretus* possess a virtually identical organization of Exon 1a and Intron 1, including insertion of the composite transposable element with Exon 1b, and testis expression of *Prl3c1-v2* but not *Prl3c1-v1* (Fig. 8D–H) (Keane 2011). The extended Intron 1 with components of the composite transposable element is also present in *M. caroli* (GenBank Accession No., KF767571); however, the organization of the composite transposable element shows marked differences and this species lacks testicular expression of either *Prl3c1-v1* or *Prl3c1-v2* (Fig. 8D–I). The more divergent *M. pahari* lacks the composite transposable element and does not express either *Prl3c1-v1* or *Prl3c1-v2* within its testes (GenBank Accession No., KF767572; Fig. 8D–H). Consistent with the Leydig cell static actions of PLP-J V2 in *M. musculus*, *M. pahari* lacks testicular *Prl3c1* expression and interestingly possesses a proportionately larger interstitial compartment within its testis when compared to *M. musculus* or *M. spretus* testes (Montoto *et al.* 2012). Collectively, these data indicate that the *Prl3c1* locus exhibited significant changes within a short evolutionary timeframe. Furthermore, comparisons of rodent amino acid sequences indicated that proteins encoded by the *Prl3c1* gene have undergone positive selection (Chuong *et al.* 2010), a measure of a rapidly evolving gene.

Regulation of *Prl3c1-v1* versus *Prl3c1-v2* expression

A conserved method for controlling regulatory elements and defense against inappropriate activation of transposable elements is via DNA methylation (Rowe and Trono 2011). Consequently, we investigated DNA methylation throughout the mouse *Prl3c1* locus, in uterine decidua (*Prl3c1-v1* expression), enriched Leydig cells isolated from the adult mouse testis, (*Prl3c1-v2* expression), and liver (negative control) using bisulfite sequencing, direct sequencing, and MultiNA-Combined Bisulfite Restriction Analysis (COBRA) (Yagi *et al.* 2008; Hayakawa *et al.* 2012). Collectively, the analyses indicated that DNA methylation status at the *Prl3c1* locus was different in decidual cells versus Leydig cells. A region approximately 2 kb upstream of the *Prl3c1-v1* transcription start site was hypomethylated in decidual cells and hypermethylated in Leydig cells, whereas the reciprocal was true for the proximal regulatory sequence immediately upstream of Exon 1b, including parts of the composite transposable element (Supplementary Fig. 2–4). The results are consistent with the idea that tissue specific DNA methylation at the *Prl3c1* locus could contribute to the differential regulation of *Prl3c1-v1* and *Prl3c1-v2*.

The two *Prl3c1* transcripts encode proteins with distinct intracellular targeting and actions

Exon 1a of the *Prl3c1* gene encodes the 5′ untranslated region (UTR) of the *Prl3c1-v1* transcript and the initial portion of the signal peptide for the PLP-J V1 protein (Alam *et al.*

2007). In contrast, Exon 1b is a noncoding exon, contributing solely to the 5′ UTR of the *Prl3c1-v2* transcript. The common Exon 2 contributes the translation initiation codon of the *Prl3c1-v2* transcript. Prominent differences in the *N*-terminal portion of the PLP-J V1 and predicted PLP-J V2 proteins prompted a comparison of their intracellular distributions in mouse Leydig cell lines (TM3, MA-10, and MLTC-1) and COS7 cells following transfection of expression vectors encoding FLAG-tagged PLP-J V1 and PLP-J V2 proteins. Western blotting of nuclear and cytosolic lysates of transfected MLTC-1 and COS7 cells demonstrated that PLP-J V1 was preferentially localized to the cytoplasm, whereas PLP-J V2 was targeted predominantly to the nucleus (Fig. 9A; Supplementary Fig. 5A). Interestingly, part of the mechanism of action of PRL in T-lymphocytes requires its nuclear translocation (Clevenger *et al.* 1991). We next determined whether ectopic expression of PLP-J V1 or PLP-J V2 affected MLTC-1 Leydig cell behavior. PLP-J V2 inhibited MLTC-1 Leydig cell proliferation, whereas PLP-J V1 did not significantly affect cell number (Fig. 9B,C). PLP-J V2 also effectively inhibited TM3, MA-10, and COS7 cell proliferation (Supplmentary Fig. 5B–D). TM3 cells possess features resembling Leydig cell progenitors, while MLTC-1 cells represent a more mature Leydig cell population (Supplementary Fig. 6A) (Mather 1980; Rahman and Huhtaniemi 2004). Ectopic expression of PLP-J V2 in MLTC-1 Leydig cells did not affect transcript levels for steroidogenic enzymes but did affect the expression of a subset of Leydig cell progenitor markers (Supplementary Fig. 6B–D). In contrast, ectopic expression of PLP-J V2 in TM3 Leydig cells stimulated *Hsd3b1* and *Hsd3b6* transcript levels, similar to LH treatment, but did not affect the expression of Leydig cell progenitor markers (Supplementary Fig. 6E–G). The absence of an effect of ectopic expression of PLP-J V1 on TM3 cell cycle or steroidogenesis has been previously reported (Yang *et al.* 2014). Thus, ectopic PLP-J V2 can alter Leydig cell behavior, but its actions are context-dependent and influenced by the developmental state of the target Leydig cell population.

To summarize, the contributions of the composite transposable element resulted in the use of an alternative exon and the production of a protein targeted to the nucleus with Leydig cell-static actions. Such actions are consistent with the testiculomegaly and Leydig cell hyperplasia observed in *Prl3c1* deficient mice (Fig. 1D–M).

Overview

The “big” testis phenotype in *Prl3c1* null mice is associated with a disruption in the HPG axis characterized by concomitant elevations in LH and testosterone and the consequences of their actions; a condition known as hypergonadotropic-hypergonadal-hyperandrogenism. Characterization of the *Prl3c1* null phenotype led to the discovery of a homeostatic setpoint control system programming testicular growth and function.

Discussion

Male fertility is dependent upon the appropriate functioning of the HPG axis (Achermann and Jameson 1999; Hedger and de Kretser 2000; Matzuk and Lamb 2008). Each functional unit within the axis works as part of a homeostatic mechanism to precisely control core testicular functions, which include testosterone and sperm production. Two important

features of the mammalian testis are evident: 1) there is a wide range of testis size and functional output across mammalian species; 2) within a species there are constraints governing testicular size and function. Dysregulated growth and function of the male gonads have consequences. Deficiencies are associated with subfertility and infertility, whereas excesses have costs to adult male health, including androgen-driven hyperplasia that can lead to neoplasia, and potentially negative consequences on social structure (Short 1997; Hedger and de Kretser 2000; Mascaro *et al.* 2013). Species-specific regulatory pathway(s) controlling this elemental reproductive process are poorly understood. We have discovered a reproductive trait with its evolutionary origins associated with gene duplication and co-optation of transposable elements. In the mouse, the size of the testis and its capacity to produce testosterone and sperm are modulated by the recruitment of a composite transposable element to the *Prl3c1* locus and its contribution to the regulation and biosynthesis of a unique protein. *Prl3c1* is a gene within the expanded PRL family. This novel control system impacts the establishment of the homeostatic setpoint determining the size and function of the testis. Although the existence of this testicular homeostatic setpoint control system is restricted to the mouse, species-specific epiregulation of the male reproductive axis may represent a universal concept, contributing to each species' reproductive success. Indeed, the testis is a common site for the expression of new and rapidly evolving genes with restricted phylogenetic distributions (Turner *et al.* 2008; Heinen *et al.* 2009; Chen *et al.* 2013). The widespread existence of species-specific modulation of the male reproductive axis evokes questions with broader implications. Are the growth and function of other organs governed by species-specific mechanisms? Are these species-specific mechanisms prone to dysregulation and do they represent potential therapeutic targets for treating disease? The existence of layers of control that are not conserved among species represents a challenge, as well as an opportunity to investigate physiological regulation and its relationship to disease.

Supplementary Material

Refer to Web version on PubMed Central for supplementary material.

Acknowledgments

We thank Dr. Jacques Tremblay (Laval University) and Drs. Gustavo Blanco, T. Rajendra Kumar, Gladys Sanchez, and Ossama Tawfik (University of Kansas Medical Center) for their advice and suggestions regarding the execution of the experimentation. We also thank Dr. Sumedha Gunewardena (University of Kansas Medical Center) for assistance with the bioinformatic analysis, Dr. Vincent Lynch (University of Chicago) for advice with the RNA POL II ChIP analysis, and Dr. Curtis Klaassen for providing the testis samples used in the mouse strain survey. We are very appreciative of the valuable feedback and advice provided by Dr. Gunter Wagner (Yale University), R. Michael Roberts (University of Missouri), Dr. Dixie Mager (University of British Columbia), and Dr. Justin Blumenstiel (University of Kansas) during various stages of the research. This work was supported by a grant from the NIH HD055523 and a National Institute of Environmental Health Sciences postdoctoral fellowship to P.B. (T32-ES007079). The University of Virginia Center for Research in Reproduction Ligand Assay and Analysis Core is supported by the Eunice Kennedy Shriver National Institute of Child Health and Human Development (NICHD)/ National Institutes of Health (Specialized Cooperative Centers Program in Reproduction and Infertility Research (SCCPIR) grant U54-HD28934.

References

Achermann JC, Jameson JL. Fertility and infertility: genetic contributions from the hypothalamic-pituitary-gonadal axis. Molecular Endocrinology. 1999; 13:812–818. [PubMed: 10379880]

Ain R, Dai G, Dunmore JH, Godwin AR, Soares MJ. A prolactin family paralog regulates reproductive adaptations to a physiological stressor. Proceedings of the National Academy of Sciences USA. 2004; 101:16543–16548.

Alam SMK, Konno T, Dai G, Lu L, Wang D, Dunmore JH, Godwin AR, Soares MJ. A uterine decidual cell cytokine ensures pregnancy-dependent adaptations to a physiological stressor. Development. 2007; 134:407–415. [PubMed: 17166917]

Alam SM, Konno T, Sahgal N, Lu L, Soares MJ. Decidual cells produce a heparin-binding prolactin family cytokine with putative intrauterine regulatory actions. Journal of Biological Chemistry. 2008; 283:18957–18968. [PubMed: 18467328]

Amory JD, Bremner W. Endocrine regulation of testicular function in men: implications for contraceptive development. Molecular and Cellular Endocrinology. 2001; 182:175–179. [PubMed: 11514052]

Bachelot A, Binart N. Reproductive role of prolactin. Reproduction. 2007; 133:361–369. [PubMed: 17307904]

Benton L, Shan LX, Hardy MP. Differentiation of adult Leydig cells. Journal of Steroid Biochemistry and Molecular Biology. 1995; 53:61–68. [PubMed: 7626518]

Birkhead, T. Promiscuity: An evolutionary history of sperm competition. Harvard University Press; Cambridge, MA: 2000.

Bronson, FH. Mammalian reproductive biology. The University of Chicago Press; Chicago, IL: 1989.

Chen H, Stanley E, Jin S, Zirkin BR. Stem Leydig cells: from fetal to aged animals. Birth Defects Research (Part C). 2010; 90:272–283. [PubMed: 21181888]

Chen S, Krinsky BH, Long M. New genes as drivers of phenotypic evolution. Nature Reviews Genetics. 2013; 14:645–660.

Chuong EB, Tong W, Hoekstra HE. Maternal-fetal conflict: rapidly evolving proteins in the rodent placenta. Molecular Biology of Evolution. 2010; 27:1221–1225.

Chuong EB, Elde NC, Feschotte C. Regulatory activities of transposable elements: from conflicts to benefits. Nature Reviews Genetics. 2017; 18:71–86.

Clevenger CV, Altmann SW, Prystowsky MB. Requirement of nuclear prolactin for interleukin-2-stimulated proliferation of T lymphocytes. Science. 1991; 253:77–79. [PubMed: 2063207]

Dai G, Wang D, Liu B, Kasik JW, Müller H, White RA, Hummel GS, Soares MJ. Three novel paralogs of the rodent prolactin gene family. Journal of Endocrinology. 2000; 166:63–75. [PubMed: 10856884]

Deb S, Hamlin GP, Roby KF, Kwok SCM, Soares MJ. Heterologous expression and characterization of prolactin-like protein-A. Identification of serum binding proteins. Journal of Biological Chemistry. 1993; 268:3298–3305. [PubMed: 8429006]

Desjardins C. Endocrine regulation of reproductive development and function in the male. Journal of Animal Science. 1978; 47:56–79. [PubMed: 122449]

Dufau ML, Catt KJ. Gonadotropic stimulation of interstitial cell functions of the rat testis in vitro. Methods in Enzymology. 1975; 39:252–271. [PubMed: 168462]

Emera D, Wagner GP. Transposable element recruitments in the mammalian placenta: impacts and mechanisms. Briefings in Functional Genomics. 2012; 11:267–276. [PubMed: 22753775]

Fawcett DW, Neaves WR, Flores MN. Comparative observations on intertubular lymphatics and the organization of the interstitial tissue of the mammalian testis. Biology of Reproduction. 1973; 9:500–532. [PubMed: 4203289]

Feschotte C, Gilbert C. Endogenous viruses: insights into viral evolution and impact on host biology. Nature Reviews Genetics. 2012; 13:283–296.

Freeman ME, Kanyicska B, Lerant A, Nagy G. Prolactin: structure, function, and regulation of secretion. Physiological Reviews. 2000; 80:1523–1631. [PubMed: 11015620]

Ge R-S, Dong Q, Sottas CM, Chen H, Zirkin BR, Hardy MP. Gene expression in rat Leydig cells during development from the progenitor to adult stage: a cluster analysis. Biology of Reproduction. 2005; 72:1405–1415. [PubMed: 15716394]

Guenet J-L, Bonhomme F. Wild mice: an ever-increasing contribution to a popular mammalian model. Trends in Genetics. 2003; 19:24–31. [PubMed: 12493245]

Hayakawa K, Nakanishi MO, Ohgane J, Tanaka S, Hirosawa M, Soares MJ, Yagi S, Shiota K. Bridging sequence diversity and tissue-specific expression by DNA methylation in genes of the mouse prolactin superfamily. Mammalian Genome. 2012; 23:336–345. [PubMed: 22193412]

Hedger MP, de Kretser DM. Leydig cell function and its regulation. Results and Problems in Cell Differentiation. 2000; 28:69–110. [PubMed: 10626295]

Hedges SB, Dudley J, Kumar S. TimeTree: a public knowledge-base of divergence times among organisms. Bioinformatics. 2006; 22:2971–2972. [PubMed: 17021158]

Heinen TJ, Staubach F, Häming D, Tautz D. Emergence of a new gene from an intergenic region. Current Biology. 2009; 19:1527–1531. [PubMed: 19733073]

Hess RA. Quantitative and qualitative characteristics of the stages and transitions in the cycle of the rat seminiferous epithelium: light microscopic observations of perfusion-fixed and plastic-embedded testes. Biology of Reproduction. 1990; 43:525–542. [PubMed: 2271734]

Hiraoka Y, Ogawa M, Sakai Y, Takeuchi Y, Komatsu N, Shiozawa M, Tanabe K, Aiso S. PLP-I: a novel prolactin-like gene in rodents. Biochimica et Biophysica Acta. 1999; 1447:291–297. [PubMed: 10542329]

Horseman ND, Zhao W, Montecino-Rodriguez E, Tanaka M, Nakashima K, Engle SJ, Smith F, Markoff E, Dorshkind K. Defective mammopoiesis, but normal hematopoiesis, in mice with a targeted disruption of the prolactin gene. EMBO Journal. 1997; 16:6926–6935. [PubMed: 9384572]

Ishibashi K, Imai M. Identification of four new members of the rat prolactin/growth hormone gene family. Biochemical and Biophysical Research Communications. 1999; 262:575–578. [PubMed: 10471365]

Jern P, Coffin JM. Effects of retroviruses on host genome function. Annual Review of Genetics. 2008; 42:709–732.

Jimenez T, McDermott JP, Sanchez G, Blanco G. Na,K-ATPase α4 isoform is essential for sperm fertility. Proceedings of the National Academy of Sciences USA. 2011; 108:644–649.

Jimenez T, Sánchez G, Wertheimer E, Blanco G. Activity of the Na,K-ATPase α4 isoform is important for membrane potential, intracellular Ca2+, and pH to maintain motility in rat spermatozoa. Reproduction. 2010; 139:835–845. [PubMed: 20179187]

Kaessmann H. Origins, evolution, and phenotypic impact of new genes. Genome Research. 2010; 20:1313–1326. [PubMed: 20651121]

Keane TM, Goodstadt L, Danecek P, White MA, Wong K, Yalcin B, Heger A, Agam A, Slater G, Goodson M, et al. Mouse genomic variation and its effect on phenotypes and gene regulation. Nature. 2011; 477:289–294. [PubMed: 21921910]

Kenagy GJ, Trombulak SC. Size and function of mammalian testes in relation to body size. Journal of Mammalogy. 1986; 67:1–22.

Kent LN, Konno T, Soares MJ. Phosphatidylinositol 3 kinase modulation of trophoblast cell differentiation. BMC Developmental Biology. 2010; 10:97. [PubMed: 20840781]

Kidwell MG, Lisch DR. Transposable elements, parasitic DNA, and genome evolution. Evolution. 2001; 55:1–24. [PubMed: 11263730]

Konno T, Graham AR, Rempel LA, Ho-Chen JK, Alam SM, Bu P, Rumi MA, Soares MJ. Subfertility linked to combined luteal insufficiency and uterine progesterone resistance. Endocrinology. 2010; 151:4537–4550. [PubMed: 20660062]

Mascaro JS, Hackett PD, Rilling JK. Testicular volume is inversely correlated with nurturing-related brain activity in human fathers. Proceedings of the National Academy of Sciences USA. 2013; 110:15746–15751.

Mather JP. Establishment and characterization of two distinct testicular epithelial cell lines. Biology of Reproduction. 1980; 23:243–252. [PubMed: 6774781]

Matzuk MM, Lamb DJ. The biology of infertility: research advances and clinical challenges. Nature Medicine. 2008; 14:1197–1213.

McLachlan RI, Wreford NG, O'Donnell L, de Kretser DM, Robertson DM. The endocrine regulation of spermatogenesis: independent roles for testosterone and FSH. Journal of Endocrinology. 1996; 148:1–9. [PubMed: 8568455]

Montoto LG, Arregui L, Sanchez NM, Gomendio M, Roldan ERS. Postnatal testicular development in mouse species with different levels of sperm competition. Reproduction. 2012; 143:333–346. [PubMed: 22187670]

Montoto LG, Magaña C, Tourmente M, Martín-Coello J, Crespo C, Luque-Larena JJ, Gomendio M, Roldan ER. Sperm competition, sperm numbers and sperm quality in muroid rodents. PLOS One. 2011; 6:e18173. [PubMed: 21464956]

Ohno, S. Evolution by gene duplication. Springer Verlag; Berlin: 1970.

Petkov PM, Cassell MA, Sargent EE, Donnelly CJ, Robinson P, Crew V, Asquith S, Haar RV, Wiles MV. Development of a SNP genotyping panel for genetic monitoring of the laboratory mouse. Genomics. 2004; 83:902–911. [PubMed: 15081119]

Rahman NA, Huhtaniemi IT. Testicular cell lines. Molecular and Cellular Endocrinology. 2004; 228:53–65. [PubMed: 15541572]

Rawn SM, Cross JC. The evolution, regulation, and function of placenta-specific genes. Annual Review of Cell and Developmental Biology. 2008; 24:159–181.

Rebollo R, Romanish MT, Mager DL. Transposable elements: an abundant and natural source of regulatory sequences for host genes. Annual Review of Genetics. 2012; 46:21–42.

Roby KF, Larsen D, Deb S, Soares MJ. Generation and characterization of antipeptide antibodies to rat cytochrome P-450 side-chain cleavage enzyme. Molecular and Cellular Endocrinology. 1991; 79:13–20. [PubMed: 1718796]

Rowe HM, Trono D. Dynamic control of endogenous retroviruses during development. Virology. 2011; 411:273–287. [PubMed: 21251689]

Sato S, Yagi S, Arai Y, Hirabayashi K, Hattori N, Iwatani M, Okita K, Ohgane J, Tanaka S, Wakayama T, et al. Genome-wide DNA methylation profile of tissue-dependent and differentially methylated regions (T-DMRs) residing in mouse pluripotent stem cells. Genes to Cells. 2010; 15:607–618. [PubMed: 20477876]

Short RV. The testis: the witness of the mating system, the site of mutation and the engine of desire. Acta Paediatrica Supplement. 1997; 422:3–7.

Simmons LW, Fitzpatrick JL. Sperm wars and the evolution of male fertility. Reproduction. 2012; 144:519–534. [PubMed: 22984191]

Soares MJ. The prolactin and growth hormone families: pregnancy-specific hormones/cytokines at the maternal-fetal interface. Reproductive Biology and Endocrinology. 2004; 2:51. [PubMed: 15236651]

Soares MJ, Konno T, Alam SMK. The prolactin family: effectors of pregnancy-dependent adaptations. Trends in Endocrinology and Metabolism. 2007; 18:114–121. [PubMed: 17324580]

Stanley EL, Johnston DS, Fan J, Papadopoulos V, Chen H, Ge RS, Zirkin BR, Jelinsky SA. Stem Leydig cell differentiation: gene expression during development of the adult rat population of Leydig cells. Biology of Reproduction. 2011; 85:1161–1166. [PubMed: 21832170]

Tilbrook AJ, Clarke IJ. Negative feedback regulation of the secretion and actions of gonadotropin-releasing hormone in males. Biology of Reproduction. 2001; 64:735–742. [PubMed: 11207186]

Toft DJ, Linzer DIH. Prolactin (PRL)-like protein J, a novel member of the PRL/growth hormone family, is exclusively expressed in maternal decidua. Endocrinology. 1999; 140:5095–5101. [PubMed: 10537137]

Turner LM, Chuong EB, Hoekstra HE. Comparative analysis of testis protein evolution in rodents. Genetics. 2008; 179:2075–2089. [PubMed: 18689890]

Yagi S, Hirabayashi K, Sato S, Li W, Takahashi Y, Hirakawa T, Wu G, Hattori N, Hattori N, Ohgane J, et al. DNA methylation profile of tissue-dependent and differentially methylated regions (T-DMRs) in mouse promoter regions demonstrating tissue-specific gene expression. Genome Research. 2008; 18:1969–1978. [PubMed: 18971312]

Yang Q, Hao J, He M, Chen M, Li G. Localization and expression patterns of prolactin-like protein-J in mouse testis. Molecular Medicine Reports. 2014; 10:255–261. [PubMed: 24806755]

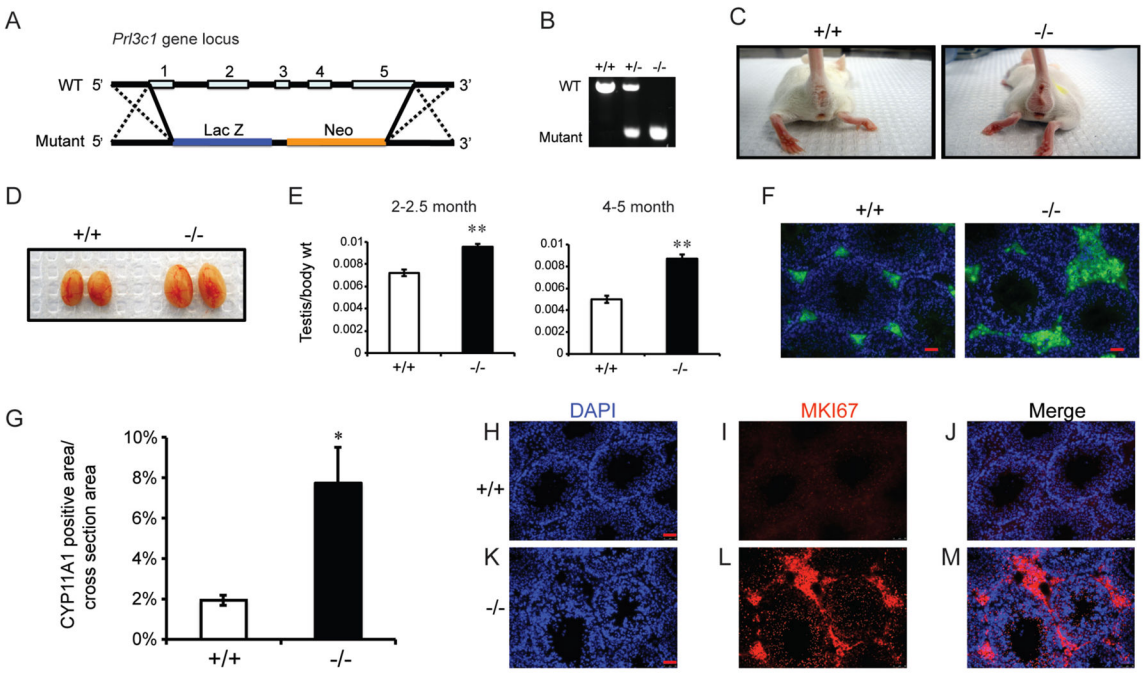

Fig. 1. *Prl3c1* mutant mice exhibit an abnormal male reproductive tract phenotype

A, Schematic of the mouse *Prl3c1* locus and the targeting construct. **B**, PCR analysis of genomic *Prl3c1* locus from wild type (+/+), heterozygous (+/−) and null (−/−) animals. **C**, Gross appearance of the scrotal area on postnatal day 21 of wild type (+/+) and *Prl3c1* null (−/−) mice. **D**, Gross appearance of adult testis of wild type and *Prl3c1* null mice. **E**, Testis-to-body weight ratio of wild type (2–2.5 months, n=14; 4–5 months, n=8) and *Prl3c1* null (2–2.5 months, n=20; 4–5 months, n=15) mice. **F**, CYP11A1 immunofluorescence staining of testis cross-sections from wild type and *Prl3c1* null mice. **G**, Quantification of CYP11A1 positive staining area/total cross-section area of wild type and *Prl3c1* null testes, n=5 testes per group. **H–M**, MKI67 immunofluorescence staining of testis cross-sections from wild type and *Prl3c1* null mice. Scale bar: 50 μm. **P*<0.05; ***P*<0.001.

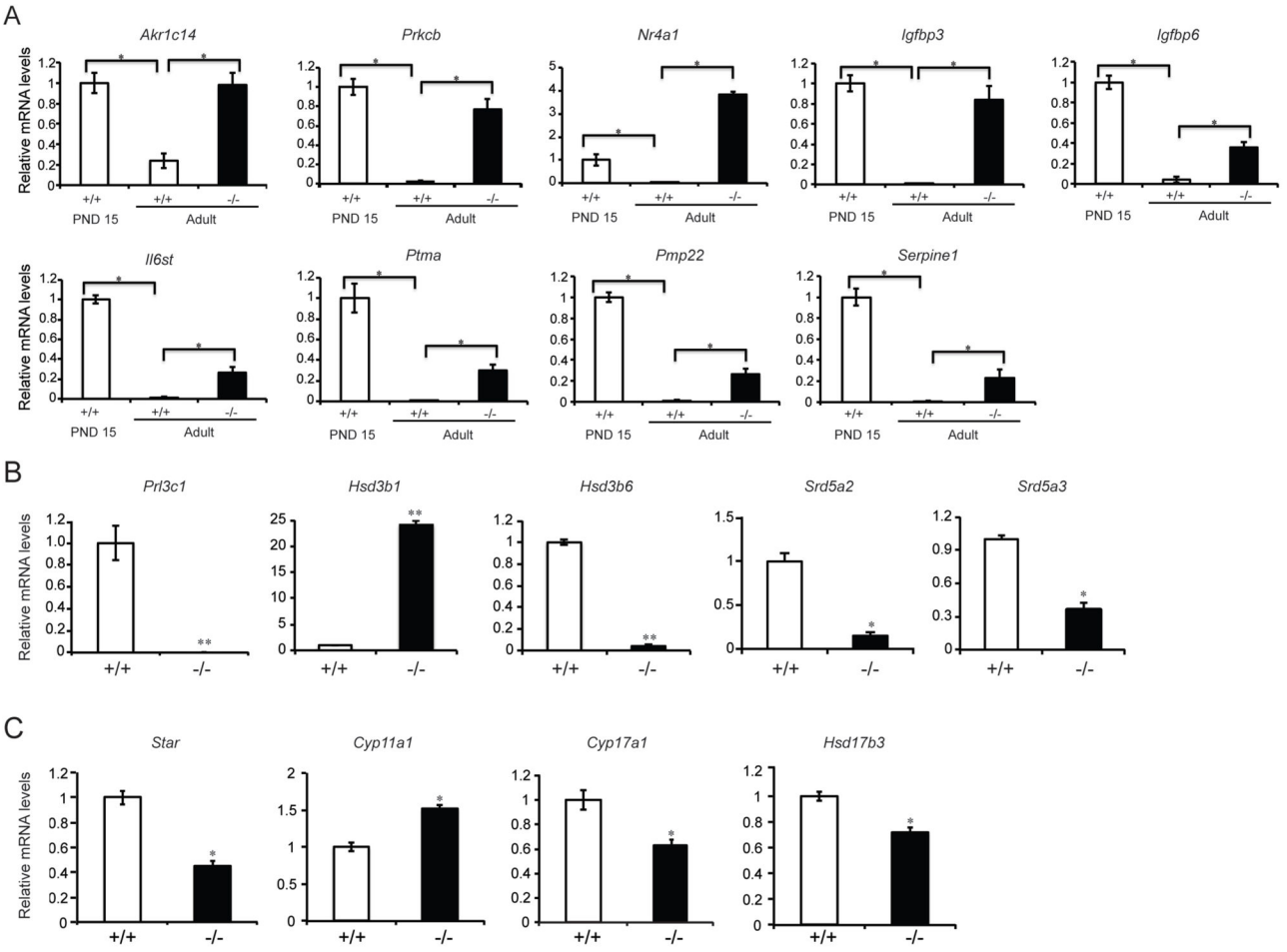

Fig. 2. Assessment of Leydig cell developmental states in wild type and *Prl3c1* null mice

A, qRT-PCR analysis of transcripts associated with the progenitor Leydig cell state in wild type postnatal day 15 (PND 15), adult (2.5–4 months) wild type and *Prl3c1* null testes. PND15 represents a transition point from progenitor to adult Leydig cells. qRT-PCR analysis of transcripts for *Prl3c1* (**B**) and transcripts encoding proteins involved in steroid hormone biosynthesis (**B,** *Hsd3b*, *Srd5a2,* and *Srd5a3*; **C,** *Star*, *Cyp11a1*, *Cyp17a1*, and *Hsd17b3*) in adult wild type and *Prl3c1* null testes (n=6; **P*<0.05, ***P*<0.001).

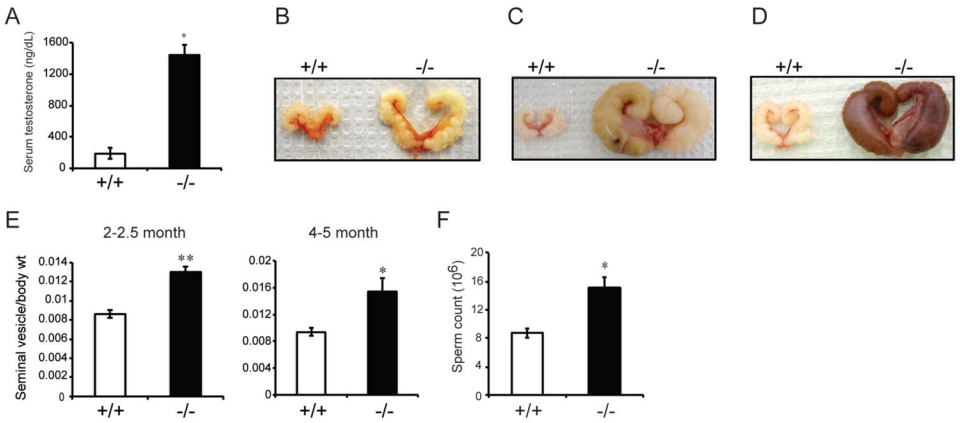

Fig. 3. Measures of testicular function in wild type and *Prl3c1* null mice

A, Serum testosterone levels from wild type (n=8) and *Prl3c1* null (n=10) male mice (3.5–4.5 months). **B**, Gross appearance of seminal vesicles from 4–5 month wild type and *Prl3c1* null mice. **C** and **D**, Gross appearance of seminal vesicles from 11–12 month wild type and *Prl3c1* null mice. **E**, Seminal vesicle-to-body weight ratio of wild type (2–2.5 months, n=14; 4–5 months, n=8) and *Prl3c1* null (2–2.5 months, n=20; 4–5 months, n=15) mice. **F**, Total sperm count of wild type and *Prl3c1* null mice (n=5 per genotype). Scale bar: 50 μm. **P*<0.05; ***P*<0.001.

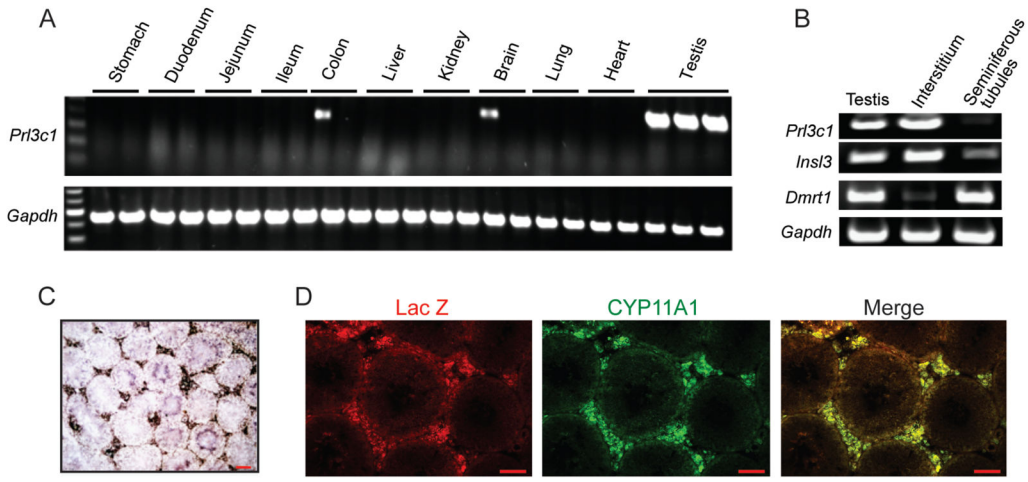

Fig. 4. *Prl3c1* transcript and the PLP-J protein are expressed in Leydig cells of the testis

A, Tissue survey (RT-PCR analysis) for *Prl3c1* transcripts in various tissues from male C57BL/6 mice. **B**, RT-PCR analysis for *Prl3c1* transcripts in testicular interstitium and seminiferous tubule compartments. *Insl3* and *Dmrt1* were included as controls for the interstitium and seminiferous tubule compartments, respectively. **C**, Immunohistochemical (IHC) staining for PLP-J on tissue sections from wild type testis. **D**, The *Prl3c1* locus is transcriptionally active in Leydig cells of mice with β-galactosidase (LacZ) knocked into the *Prl3c1* locus. Left panel: LacZ reporter activity; middle panel: immunofluorescence staining for CYP11A1; right panel: merged image of LacZ and CYP11A1 staining. LacZ reporter activity was localized to CYP11A1 positive Leydig cells in mice. Scale bar: 250 μm.

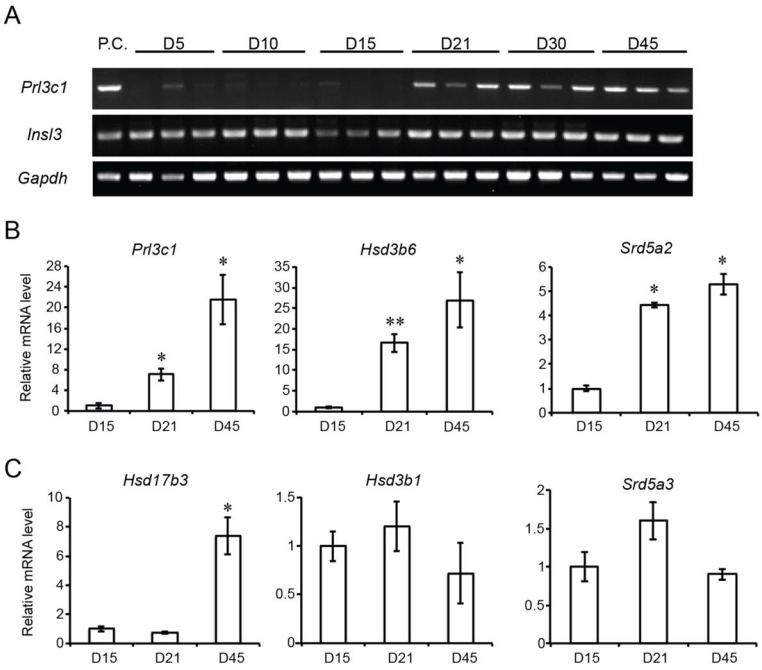

Fig. 5. Ontogeny of *Prl3c1* and steroidogenic enzyme transcripts in testes of wild type mice

A, RT-PCR analysis of *Prl3c1* transcript expression in testes from postnatal days 5 to 45 (n=3 per day). Positive control (P.C.) is adult testis. *Insl3* and *Gapdh* transcript analyses were used as internal controls. **B and C,** qRT-PCR measurements of transcripts for *Prl3c1* (**B**) and transcripts encoding proteins involved in steroid hormone biosynthesis (**B,** *Hsd3b* and *Srd5a2*; **C,** *Hsd17b3, Hsd3b1, Srd5a3*) in testes at postnatal days 15 (D15), 21 (D21), and 45 (D45) (n=6, **P*<0.05, ** *P*<0.001, compared to D15).

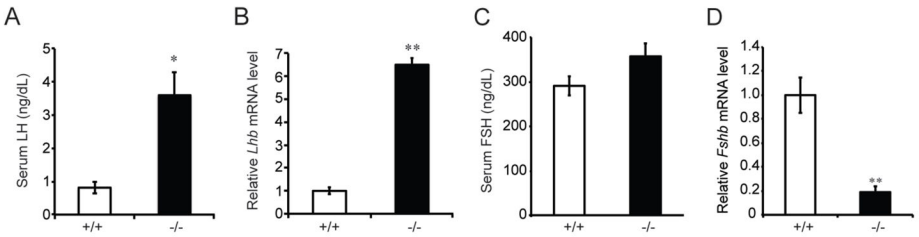

Fig. 6. The testicular homeostatic setpoint control system includes the pituitary

A, Serum LH levels in wild type (n=8) and *Prl3c1* null (n=10) adult male mice. **P*<0.05. **B**, *Lhb* transcript levels in pituitaries of wild type (n=5) and *Prl3c1* null (n=7) adult male mice analyzed by qRT-PCR. ***P*<0.001. **C**, Serum FSH levels in wild type (n=18) and *Prl3c1* null (n=18) adult male mice. **D**, *Fshb* transcript levels in pituitaries of wild type (n=5) and *Prl3c1* null (n=7) adult male mice analyzed by qRT-PCR. ***P*<0.001.

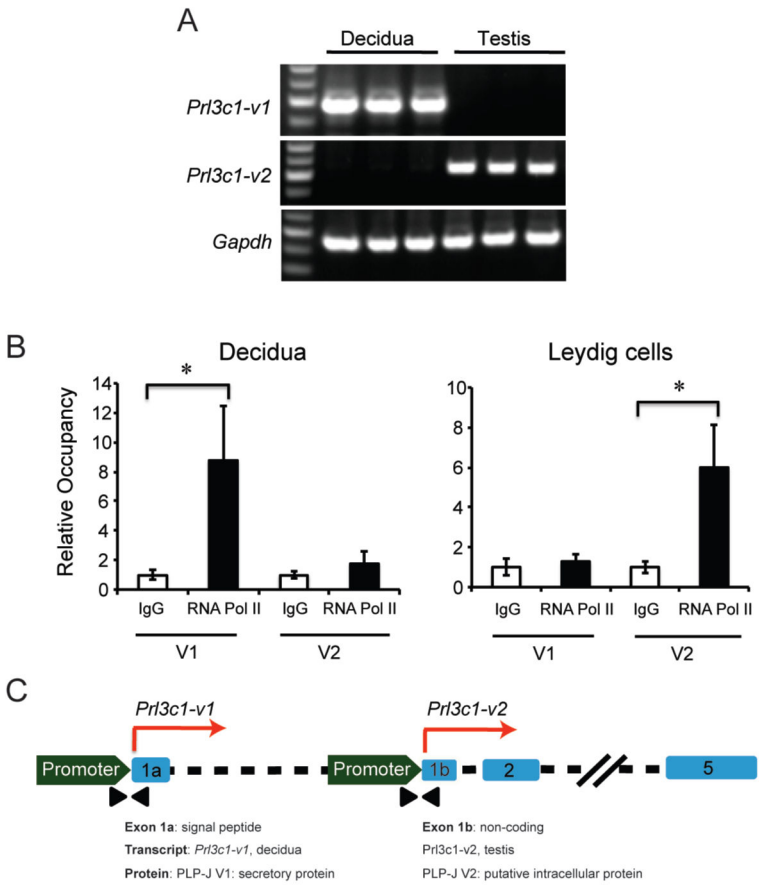

Fig. 7. The *Prl3c1* gene is a template for two transcripts with distinct tissue expression patterns

A, *Prl3c1* transcript-specific RT-PCR analysis revealed tissue-restricted expression patterns for *Prl3c1-v1* (decidua) and *Prl3c1-v2* (testis). **B**, ChIP-qPCR analysis for RNA POL II at regions proximal to Exons 1a of *Prl3c1-v1* (V1) and 1b of *Prl3c1-v2* (V2) in decidua and Leydig cells. Locations of primer sets used in ChIP-qPCR are depicted as arrowheads shown in panel **C** (n=4, **P*<0.05 compared to IgG control). **C**, Schematic representation of transcription start sites for *Prl3c1-v1* (decidua) and *Prl3c1-v2* (Leydig cells) as determined by 5′RACE (see also Supplementary Fig. 1A,B).

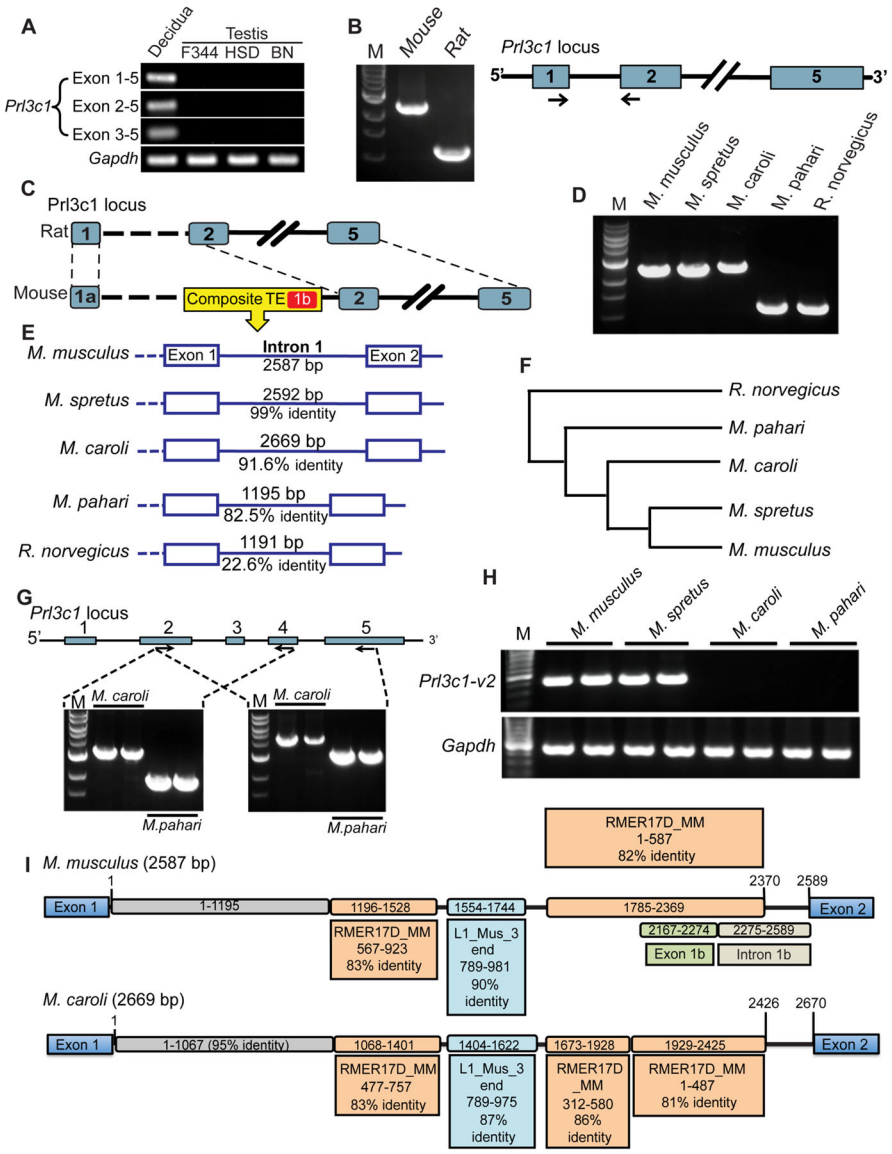

Fig. 8. Origin and species specificity of the testicular homeostatic setpoint control system

A, RT-PCR analysis for *Prl3c1* transcripts with primers targeting various exons of the rat *Prl3c1* gene in testes of Fischer 344 (F344), Holtzman Sprague Dawley (HSD) and Brown Norway (BN) rats. Decidua tissue (HSD, gestation day 7.5) was included as a positive control. **B**, PCR amplification of the first intron of the *Prl3c1* gene from the mouse (C57BL/6) and rat (BN). Schematic diagram of exon-intron structure indicates the locations of the primers used for amplification. **C**, Schematic comparison of the mouse and rat *Prl3c1* genes reveals a longer first intron in the mouse due to the insertion of a composite transposable element (TE), which contains Exon 1b of *Prl3c1-v2*. **D**, PCR amplification of the first introns of the *Prl3c1* genes from *M. musculus, M. spretus, M. caroli, M. pahari,* and *R. norvegicus*. **E**, Schematic representations of the first introns of the *Prl3c1* genes from *M. musculus, M. spretus, M. caroli, M. pahari,* and *R. norvegicus*. Sequence identity comparisons are with the *M. musculus* sequence. **F**, Phylogenetic tree based on the

nucleotide sequences for the first introns of *Prl3c1* genes from *M. musculus*, *M. spretus*, *M. caroli*, *M. pahari*, and *R. norvegicus*. **G**, Primer validation for *M. caroli* and *M. pahari*. Schematic diagram indicates the locations of the two sequence-specific primer sets used for detection of *Prl3c1* transcripts in testes from *M. caroli* and *M. pahari*. Primer sequences were based on partially sequenced coding regions of *M. caroli* (GenBank Accession No., KJ125427) and *M. pahari* (GenBank Accession No., KJ125428) *Prl3c1* genes and validated by PCR amplification of corresponding *Prl3c1* genomic regions with genomic DNA from these species. **H**, RT-PCR analysis for *Prl3c1* transcripts in testes of *M. musculus, M. spretus, M. caroli,* and *M. pahari.* Two sets of sequence specific primers were used for *M. caroli* and *M. pahari*. **I**, Annotated schematic of the first intron of *Prl3c1* from *M. musculus* and *M. caroli*. Note the prominent differences in the organization of RMER17D in *M. musculus* versus *M. caroli*.

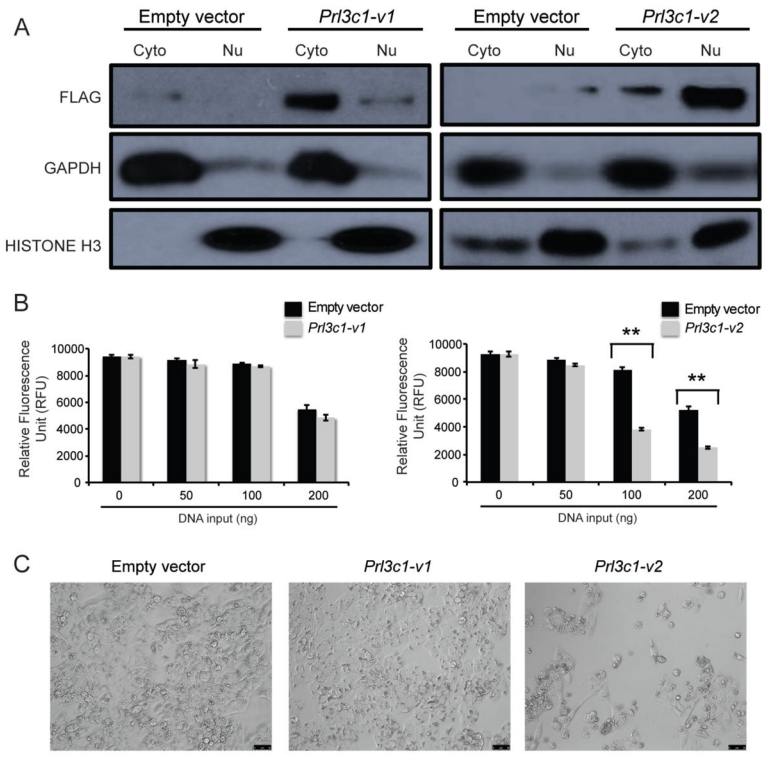

Fig. 9. Intracellular distribution and distinct functions of PLP-J V1 versus PLP-J V2

FLAG-tagged PLP-J V1 and FLAG-tagged PLP-J V2 were ectopically expressed in MLTC-1 Leydig cells or COS7 cells (1 μg/ml). Cells transfected with an empty vector were used as a control (1 μg/ml). **A**, Subcellular fractionation followed by western blotting for FLAG (Cyto: cytoplasm; Nu: nucleus). Western blotting for GAPDH and Histone H3 were used to monitor the integrity of the cytoplasmic and nuclear preparations, respectively. **B**, Effects of ectopic expression of *Prl3c1-v1* (left panel) or *Prl3c1-v2* (right panel) on MLTC-1 Leydig cell numbers following 72 h of culture. Cells were cultured in 96 well plates with 0.1 ml of medium/well (n=6, $^{**}P<0.001$ compared to empty vector control). **C**, Representative images of MLTC-1 cells transfected with empty vector, *Prl3c1-v1*, or *Prl3c1-v2* (1 μg/ml) following 72 h of culture.